THE JOURNAL OF BIOLOGICAL CHEMISTRY
Vol. 273, No. 52, Issue of December 25, pp. 35161–35169, 1998
Printed in U.S.A.

Molecular Mechanism of Basic Calcium Phosphate Crystal-induced Activation of Human Fibroblasts

ROLE OF NUCLEAR FACTOR κB, ACTIVATOR PROTEIN 1, AND PROTEIN KINASE C*

(Received for publication, May 21, 1998, and in revised form, September 3, 1998)

Geraldine M. McCarthy‡, James A. Augustine§, Albert S. Baldwin¶, Pamela A. Christopherson, Herman S. Cheung‖, Pamela R. Westfall, and Robert I. Scheinman**

*From the §Department of Medicine (Rheumatology), Medical College of Wisconsin and the Blood Research Institute, Milwaukee, Wisconsin 53226, the ¶Lineberger Comprehensive Cancer Institute, University of North Carolina, Chapel Hill, North Carolina 27599, the ‖Department of Medicine (Arthritis), University of Miami School of Medicine and Geriatric Research, Education and Clinical Center, Veterans Administration Medical Center, Miami, Florida 33125, and the **School of Pharmacy, University of Colorado Health Sciences Center, Denver, Colorado 80262*

Synovial fluid basic calcium phosphate (BCP) crystals are markers of severe joint degeneration in osteoarthritis. BCP crystals cause mitogenesis of articular cells and stimulate matrix metalloprotease production, thus promoting degradation of articular tissues. Previous work suggested that BCP crystal-induced cell activation required intracellular crystal dissolution, induction of proto-oncogene expression, and activation of signal transduction pathways involving protein kinase C and mitogen-activated protein kinases. Here we further elucidate the mechanisms of BCP crystal-induced cell activation as BCP crystals activate transcription factors nuclear factor κB and activator protein 1 in human fibroblasts. We confirm the role of protein kinase C in BCP crystal-induced mitogenesis in human fibroblasts. In contrast, we demonstrate that BCP crystals do not activate signal transduction pathways involving protein tyrosine kinases or phosphatidylinositol 3-kinase. These data further define the mechanism of cell activation by BCP crystals and confirm its selectivity, an observation that may have therapeutic implications.

Synovial fluid basic calcium phosphate (BCP)[1] (hydroxyapatite, octacalcium phosphate, and tricalcium phosphate) crystals are common in osteoarthritis (OA) and are associated with severe degenerative arthropathies (1). The prevalence of BCP crystals in synovial fluid from patients with knee OA is between 30 and 60%, and their presence correlates strongly with radiographic evidence of cartilage degeneration (2). Larger joint effusions are seen in affected joints when compared with joint fluid from OA knees without BCP crystals (3).

Clinical and pathological studies have demonstrated that synovial lining proliferation of varying degrees is associated with BCP crystals in osteoarthritis (4). BCP crystals themselves are at least partly responsible for such proliferation since they stimulate cell replication *in vitro* (5). Increased cellularity in the synovial lining enhances the capacity for secretion of cytokines, which may promote chondrolysis. Noninflammatory destruction of matrix-rich articular structures including cartilage, ligament, and tendon is also characteristic of BCP crystal deposition (1). BCP crystals promote tissue damage by induction of matrix metalloprotease (MMP) synthesis and secretion. Since there are no available drugs to inhibit deposition or affect reabsorption of these crystals, prevention of the biological consequences of the destructive processes initiated by BCP crystals is an attractive therapeutic strategy.

The *in vitro* effects of BCP crystals emphasize their pathogenic potential. BCP crystals induce mitogenesis in cultured fibroblasts (5, 6). However, mechanisms by which BCP crystals induce mitogenesis have been incompletely studied. Endocytosis and intracellular dissolution of the crystals, producing an elevated cytoplasmic calcium concentration, are important (7). BCP crystals activate a protein kinase signal transduction pathway involving p42 and p44 mitogen-activated protein (MAP) kinases (8). Current data suggest that BCP crystals enhance phospholipase C activity in synovial fibroblasts (9). If BCP crystals increase phospholipase C activity, resultant diacylglycerol accumulation followed by increased protein kinase C (PKC) activity should ensue. This postulate is supported in a study by Mitchell *et al.* (6) who found that BCP crystal-induced mitogenesis in Balb/c/3T3 fibroblasts was inhibited when PKC was down-regulated using the tumor-promoting phorbol ester, 12-*O*-tetradecanoyl-phorbol 13-acetate (TPA), an analogue of diacylglycerol. Another index of PKC activation is translocation of the enzyme from the cytosolic compartment to the membrane compartment of the cell, and we have shown increased membrane-associated PKC activity in porcine chondrocytes treated with BCP crystals (10). These data suggest that the mitogenic response to BCP crystals involves activation of PKC. However, BCP crystal-induced activation of PKC in human cultures has not been reported.

* This work was supported by grants from the National Arthritis Foundation, American Federation for Aging Research, National Institutes of Health Grants AR-01953 (to G. M. C.) and AR-38421 (to H. S. C.), the Lupus Foundation of America, the Cancer League of Colorado, and the American Association of Colleges of Pharmacy (to R. I. S.). The costs of publication of this article were defrayed in part by the payment of page charges. This article must therefore be hereby marked "*advertisement*" in accordance with 18 U.S.C. Section 1734 solely to indicate this fact.

‡ To whom correspondence should be addressed: Dept. of Clinical Pharmacology, The Royal College of Surgeons in Ireland, 123, St. Stephens Green, Dublin 2, Ireland. Tel.: 353-1-4782165; Fax: 353-1-4022453.

[1] The abbreviations used are: BCP, basic calcium phosphate; DMEM, Dulbecco's modified Eagle's medium; FBS, fetal bovine serum; HF, human fibroblasts; PKC, protein kinase C; TPA, 12-*O*-tetradecanoyl-phorbol-13-acetate; EMSA, electrophoretic mobility shift analysis; PAGE, polyacrylamide gel electrophoresis; PDGF, platelet-derived growth factor; PtdIns, phosphatidylinositol; PI3K, phosphatidylinositol 3-kinase; PI3 kinase, phosphatidylinositol 3-kinase; NF-κB, nuclear factor κB; PTK, protein tyrosine kinases; OA, osteoarthritis; PDGF, platelet-derived growth factor; CPPD, calcium pyrophosphate dihydrate; TRE, TPA response element; IL-1β, interleukin-1β; MMP, matrix metalloprotease; TBS, Tris-buffered saline; AP-1, activator protein 1; MAP, mitogen-activated protein; PBS, phosphate-buffered saline; HA1004, *N*-(2-guanidinoethyl)-5-isoquinolinesulfonamide hydrochloride; H7, 1-(5-isoquinolinesulfonyl)-2-methylpiperazine dihydrochloride.

A potentially important pathway of crystal-induced cell activation involves transcription factor, nuclear factor κB (NF-κB). Present in the cytoplasm of most cell types, NF-κB is critical to many signal transduction pathways, including those leading to cell replication and oncogenesis, and is induced during the G_0 to G_1 transition of mitogenesis in murine fibroblasts (11). The best characterized form of NF-κB consists of a heterodimer composed of a 50-kDa (p50) and a 65-kDa (p65) (also called RelA) subunit (12). In unstimulated cells, NF-κB is found in the cytoplasm bound to IκB (inhibitor κB), a member of a family of inhibitor proteins that prevents it from entering the nucleus. When cells are exposed to inducers of NF-κB, two serine residues of IκB are phosphorylated by specific IκB kinases causing its rapid degradation by the 26 S proteasome and loss of NF-κB inhibitory activity (13). NF-κB is thus released to translocate to the nucleus and activate transcription of target genes. BCP crystals induce mitogenesis, but their ability to activate NF-κB has not previously been studied.

Alternatively, crystal-induced mitogenesis may derive from other pathways. The cellular effects of many growth-promoting agents are mediated by high affinity receptor protein tyrosine kinases (PTK) (14). In mammalian cells, the binding of ligand to the extracellular domain induces tyrosine phosphorylation of the cytoplasmic domain. This leads to recruitment and downstream activation of a number of common signaling molecules including PTK and phosphatidylinositol 3-kinase (PI3 kinase) (15). Phosphoinositides play a key role in signal transduction, and the 3-phosphoinositide pathway has been implicated in growth factor-dependent mitogenesis (16). Production of 3-phosphoinositides requires PTK-mediated recruitment and activation of PI3 kinase (15). Calcium pyrophosphate dihydrate (CPPD) and monosodium urate crystals induce protein tyrosine phosphorylation in human neutrophils (17). PI3 kinase is also involved in CPPD and monosodium urate crystal-induced neutrophil activation (18), but the role of either in BCP crystal-induced activation of neutrophils, fibroblasts, or chondrocytes has not been reported.

Transduction pathways resulting in protease synthesis and secretion are likely active in BCP crystal-induced arthritis. Probable effectors of tissue damage from BCP crystals are MMPs, including collagenase-1 (MMP-1), stromelysin (MMP-3), 92-kDa gelatinase (gelatinase B/MMP-9), and collagenase-3 (MMP-13) (19–21). The collagenase promotor contains a *cis* element termed the TPA response element (TRE), which is involved in increased transcription in response to agonists including tumor necrosis factor α and phorbol esters (22, 23). Increased transcription through the TRE depends on the transcription factor activator protein-1 (AP-1), a heterodimer composed of the protein products of c-*fos* and c-*jun*, both primary response genes, which interact to stimulate transcription of AP-1-responsive genes. BCP crystals induce c-*fos* and c-*jun* mRNA accumulation in human fibroblasts (HF) and inhibitors of protein synthesis such as cycloheximide block BCP crystal induction of MMP mRNA (19, 24). This suggests that synthesis of a transactivating complex containing Fos and Jun proteins, such as AP-1, is necessary for BCP crystal induction of MMPs.

In the present study, we demonstrate that the mitogenic response to BCP crystals is associated with PKC activation in HF and NF-κB induction in Balb/c/3T3 and HF. We confirm that BCP crystals induce the transcription factor AP-1, and we show that the PKC inhibitor, staurosporine, inhibits BCP crystal induction of c-*fos*, but not c-*jun*, mRNA in HF. In contrast, we show that BCP crystals do not activate PI3 kinase or tyrosine kinases confirming that cell activation by BCP crystals is selective in mechanism.

EXPERIMENTAL PROCEDURES

Materials

The monoclonal anti-PKC antibody MC-5, which recognizes α and β forms of PKC, was from Amersham Pharmacia Biotech. The polyclonal antibody raised in rabbits against IκBα, was from Rockland, Inc. (Gilbertsville, PA). The polyclonal anti-peptide antibody against c-Fos (c-Fos(K-25)XTransCruz™) was from Santa Cruz Biotechnology (Santa Cruz, CA). The murine monoclonal anti-PI3K antibody against human p85α and the anti-phosphotyrosine antibody, 4G10, were from Upstate Biotechnology, Inc. (Lake Placid, NY). Biotin-labeled goat anti-rabbit IgG and peroxidase-labeled streptavidin were from Kirkegaard & Perry Laboratories, Inc. (Gaithersburg, MD). Enhanced chemiluminescence was performed using a kit from Amersham Corp. (Buckinghamshire, UK). Tritiated thymidine (50 Ci/mmol) was from Amersham Pharmacia Biotech, and [α-^{32}P]dCTP and [α-^{32}P]dATP were from ICN Pharmaceuticals, Inc. (Irvine, CA). The AP-1 probe was the AP-1 consensus oligonucleotide (5′-CGCTTGATGACTCAGCCGGAA-3′) from Santa Cruz Biotechnology (Santa Cruz, CA). The mutant AP-1 probe was also from Santa Cruz Biotechnology. The c-*fos* probe was a 1.3-kilobase pair *Pst*I v-*fos* fragment from the pfos-1/plasmid supplied by I. Verma (Salk Institute, San Diego, CA) (25). The c-*jun* probe was a 0.9-kilobase pair *Bam*HI/*Pst*I insert from the RSV-cJ plasmid, supplied by Dr. Michael Karin (University of California, San Diego) (26). The pHcGAP plasmid containing glyceraldehyde-3-phosphate dehydrogenase cDNA (27) was from the American Type Culture Collection (27). Staurosporine was from Kamiya Biomedical Co. (Thousand Oaks, CA). H7 (1-(5-isoquinolinesulfonyl)-2-methylpiperazine dihydrochloride) and HA1004 (*N*-(2-guanidinoethyl)-5-isoquinolinesulfonamide hydrochloride) were from Seikagaku America, Inc. (St. Petersburg, FL) Bisindoylmaleimide-1 was from Calbiochem. Human recombinant platelet-derived growth factor (PDGF)-BB was from Austral Biologics (San Ramon, CA). Recombinant human interleukin-1β (IL-1β) was from R & D Systems (Minneapolis, MN). Phosphatidylinositol (PtdIns) and phosphatidylserine were from Avanti Polar Lipids (Alabaster, AL). PtdIns, PtdIns(4)P, and PtdIns(4,5)P_2 were from Calbiochem. 12-*O*-Tetradecanoylphorbol 13-acetate (TPA) and latex beads (particles 0.46 μm in diameter) were from Sigma. Diamond dust (particles 1–5 μm long) was obtained from A. Landau Co. (Philadelphia, PA). Colorado calf serum was from the Colorado Serum Co (Denver, CO). Bovine calf serum, fetal bovine serum (FBS), Hanks' buffered saline solution, and DMEM were from Life Technologies, Inc.

Cell Culture

A model system of human foreskin fibroblast (HF) cultures was used for these experiments since HF responses to BCP crystals have been shown to be similar to those of synovial fibroblasts (5). HF cultures were established from explants and transferred as described previously (28). They were grown and maintained in DMEM supplemented with 10% FBS containing 1% penicillin, streptomycin, and Fungizone (PSF). All experiments were performed on confluent cell monolayers that had been rendered quiescent by removing the media, washing with DMEM alone, and subsequently incubating in DMEM containing 0.5% FBS and 1% PSF for 24 h. All cultures used were 3rd or 4th passage cells.

Balb/c/3T3 (American Type Culture Collection, Rockville, MD) cultures were grown and maintained in DMEM with 10% Colorado calf serum and 1% penicillin/streptomycin. When approximately 70% confluent, cultures were rendered quiescent by incubating in DMEM containing 0.5% Colorado calf serum for 24 h prior to experiments.

NIH 3T3 cells (American Type Culture Collection) were cultured in DMEM supplemented with 10% bovine calf serum and 1% penicillin/streptomycin.

Determination of Mitogenesis by Uptake of [^{3}H]Thymidine

Cells were grown to confluence in 24-well plates and rendered quiescent by incubation in 0.5% FBS for 24 h. [^{3}H]Thymidine (1 μCi/ml) was added to the wells 23 h after the addition of 10% FBS, TPA (200 nM), or BCP crystals (18 μg/cm^2) in the presence or absence of varying concentrations of staurosporine and pulse-labeled for 1 h. Control cultures were in 0.5% FBS with or without varying concentrations of staurosporine. The cells were then washed 3 times with phosphate-buffered saline (PBS), and macromolecules were precipitated with 5% trichloroacetic acid solution. The precipitate was washed again with PBS and dissolved in 1 ml 0.1 N NaOH, 1% SDS. Levels of trichloroacetic acid-precipitable ^{3}H were determined in triplicate, using a liquid scintillation counter (Packard Instruments, Downers Grove, IL).

Crystal Synthesis and Preparation

BCP crystals were synthesized by a modification of published methods (29). Mineral prepared by this method has a calcium/phosphate molar ratio of 1.59 and contains partially carbonate-substituted hydroxyapatite with admixed octacalcium phosphate shown by Fourier transform infrared spectroscopy. The crystals were crushed and sieved to yield 10–20-μm aggregates, which were sterilized and rendered pyrogen-free by heating at 200 °C for 90 min. Heating to 200 °C did not alter the crystal character or the relationship of hydroxyapatite and octacalcium phosphate, as confirmed by x-ray diffraction and Fourier transform infrared spectroscopy. Crystals were weighed and suspended by sonication in Dulbecco's modified Eagle's medium (DMEM). The crystal suspension was sonicated again just prior to use. The amounts of crystals used were determined based on our previous studies of dose-response relationships between BCP crystals and the mitogenic response (5). In those studies, maximal mitogenic responses were achieved with BCP levels of 50–100 μg/ml. These levels are equivalent to concentrations of BCP crystals found in pathologic joint fluids.

Extract Preparation

Cells were washed in PBS and lysed in E buffer (0.3% Nonidet P-40, 10 mM Tris, pH 8.0, 60 mM NaCl, 1 mM EDTA, 1 mM dithiothreitol, 1 mM phenylmethylsulfonyl fluoride (PMSF)) by 5 min of incubation on ice. Nuclei were pelleted by spinning for 5 min at 2,500 rpm at 4 °C in an Eppendorf microcentrifuge, and the supernatant was saved as the cytoplasmic extract prior to SDS-PAGE through 10% polyacrylamide gels (30). Glycerol was added to cytoplasmic extracts to a final concentration of 20%, after which the extracts were stored at −80 °C until use. Nuclear extracts were washed in buffer E without Nonidet P-40 and resuspended in 40 μl of C buffer (20 mM HEPES, pH 7.9, 0.75 mM spermidine, 0.15 mM spermine, 0.2 mM EDTA, 2 mM EGTA, 2 mM dithiothreitol, 20% glycerol, 1 mM PMSF). NaCl was added to a concentration of 0.4 M, and the nuclei were gently shaken for 10 min at 4 °C. The nuclei were then pelleted by spinning for 10 min at 14,000 rpm at 4 °C in an Eppendorf microcentrifuge, and the nuclear extract supernatant was stored at −70 °C until use. The protein content of cell extracts was determined using the method of Bradford (Bio-Rad) (31).

DNA Binding Reactions and Electrophoretic Mobility Shift Analysis (EMSA)

EMSA was performed using a radiolabeled probe, UV 21, designed for cross-linking studies. This probe is derived from a template oligonucleotide UV1 (CAGGGCTGGGGATTCCCCATCTCCACAGTTTCACTTC) corresponding to bases −178 to −141 of the region 1 enhancer of the *H-2K*^{b} gene which contains a strong κB motif. UV1 was annealed to primer UV2 (GAAGTGAAAC-TGTGG) and extended with Klenow fragment in the presence of [α-^{32}P]dCTP as described previously (32). The AP-1 probe is described under "Materials." Binding reactions were performed by first incubating 2 μg of nuclear extract with 1 μg of poly(dI-dC) in binding buffer (10 mM Tris, pH 7.7, 50 mM NaCl, 20% glycerol, 1 mM dithiothreitol, 0.5 mM EDTA) for 10 min at room temperature. Approximately 10,000 cpm of probe was then added and allowed to bind for approximately 30 min. Some nuclear extracts were treated with IκB (recombinant IκBα expressed in *Escherichia coli* and purified using histidine tags) prior to addition of the UV 21 probe. The reaction mix was then loaded onto native 5% acrylamide gels, prepared with 0.25× TBE (22.3 mM Tris, 22.3 mM borate, 0.5 mM EDTA). Supershift experiments were performed by incubating binding reaction mixes with 1 μl of antiserum for 15 min at room temperature. The polyclonal antibody against p50 (Ab1141) is generated in rabbits and is raised against a peptide fragment made from amino acids 2–15 of human p105. The anti-p65 antibody (Ab5192) is polyclonal antisera against the C terminus of human p65. Gels were analyzed either by autoradiography or with a PhosphorImager (Molecular Dynamics).

Northern Blot Analysis

Northern blot analysis of total cellular RNA was used to study the expression of c-*fos* and c-*jun* mRNA in HF after stimulation with BCP crystals in the presence or absence of the PKC inhibitor staurosporine. Confluent, quiescent monolayer cultures of HF in 100-mm plates were washed twice with cold PBS 24 h after treatment. Total RNA was recovered by precipitation with 4 M LiCl as described by Cathala *et al.* (33). Five micrograms of total cellular RNA was fractionated on a 1.2% agarose-formaldehyde gel; ribosomal RNA was visualized with ethidium bromide, and the fractionated RNA was transferred to nitrocellulose filters (34). Hybridization of the filters with DNA probes was performed overnight at 42 °C. Probes were labeled using the random primer method, and [α-^{32}P]dATP, to a specific activity of $>5 \times 10^8$ cpm/μg (35). The filters were washed at a maximal stringency of 0.25× standard saline citrate (SSC, 1× SSC = 0.15 M sodium chloride, 0.015 M sodium citrate, pH 7.0) at 60 °C for 30 min. Autoradiography was performed with Kodak XAR-5 film (Eastman Kodak Co.), and signal intensity was quantified by scanning laser densitometry (LKB Instruments, Stockholm, Sweden).

PKC Translocation

Confluent cultures of HF grown in 100-mm plates were washed twice in cold PBS and then harvested in 1.5 ml of translocation buffer (20 mM Tris-HCl, pH 7.5, 2 mM EDTA, 0.5 mM EGTA, 0.2 mM PMSF, 10 μg/ml leupeptin, 10 μg/ml aprotinin, 0.33 M sucrose) (36). Cells were sonicated on ice for 15 s and then centrifuged at 100,000 × *g* for 45 min. The supernatant was used as the cytosolic fraction. The pellet was then dissolved in 0.5 ml of translocation buffer containing Triton X-100 (0.1% w/v), shaken at 4 °C overnight, and then centrifuged at 100,000 × *g* for 45 min. The supernatant was used as the membrane fraction. Samples (20 μl) of cytosolic and membrane fractions were subjected to SDS-PAGE in 10% polyacrylamide gels.

PKC Activity Assay

Plates were washed 2 times in cold PBS and then scraped into 1 ml of buffer A (0.3 M sucrose, 50 mM Tris-HCl, pH 7.5, 5 mM EDTA, 10 mM EGTA, 0.3% β-mercaptoethanol, 0.1 mM PMSF, 10 mg/ml pepstatin, 10 mg/ml soybean trypsin inhibitor) and sonicated for 30 s. The cell lysate was then centrifuged at 100,000 × *g* for 45 min, and the supernatant was removed. The pellet was resuspended in 1 ml of buffer A containing 1% Triton X-100 and then applied to 200 ml of DEAE-Sepharose minicolumns equilibrated in buffer B (buffer A without sucrose). The columns were then washed with 1 ml of buffer B and eluted with 1 ml of buffer C (buffer B + 0.15 M NaCl). Prior experiments determined that 0.15 M NaCl eluted the majority of the PKC activity. 25 ml samples were then assayed for PKC activity using a PKC assay kit (Amersham Pharmacia Biotech). This assay is a modification of the mixed micelle assay and utilizes a peptide that is specifically phosphorylated on threonine by PKC (37, 38). Assay conditions and separation of the phosphorylated peptide were as described in the instructions supplied with the kit.

Western Blotting

After electrophoresis, proteins were electrophoretically transferred to nitrocellulose membranes overnight at 4 °C. After transfer, the membranes were blocked in 2.5% non-fat dry milk in Tris-buffered saline (TBS) (20 mM Tris, 500 mM NaCl, pH 7.5). The membranes were washed twice with Tween 20 wash solution (20 mM Tris, 500 mM NaCl, 0.05% Tween 20) (TTBS). The membranes were then incubated for 1 h with antibody buffer (0.1% non-fat dry milk-TTBS) containing a 1:500 or 1:1000 dilution of primary antibodies. The blots were then washed with TTBS and incubated with a 1:1000 dilution of biotin-conjugated goat anti-mouse or anti-rabbit IgG for 1 h. The blots were washed with TTBS and incubated with a 1:1000 dilution of alkaline phosphatase/streptavidin for 1 h. Membranes were washed twice with TTBS and once with TBS. Immunoreactive bands were detected using enhanced chemiluminescence reagents (ECL) (Amersham Pharmacia Biotech).

Protein Tyrosine Kinase and PI3 Kinase Analysis

Lysis and Immunoprecipitation—Adherent fibroblasts in 100-mm plates were solubilized in 1 ml of lysis buffer (50 mM HEPES, pH 7.4), 150 mM NaCl, 10 mM NaCl, 10 mM EDTA, 200 mM NaF, 20 mM NaP_2O_7, 10% glycerol, 1% Triton X-100) supplemented with 20 μg/ml aprotinin, 20 μg/ml leupeptin, 1 mM benzamidine, 1 mM Na_3VO_4, and 1 mM PMSF. The Triton-insoluble fraction was pelleted by centrifugation at 15,000 × *g* for 4 min at 4 °C. The supernatants were incubated with equal amounts of the appropriate antibodies for 2 h at 4 °C, and the antibody immunoprecipitates were collected on protein G-agarose for an additional hour. Immune complexes were washed twice with lysis buffer, twice with 100 mM Tris, pH 7.6, 500 mM LiCl, and twice with TNE buffer (10 mM Tris, pH 7.4, 100 mM NaCl, 1 mM EDTA). All washes were supplemented with 20 μg/ml aprotinin, 20 μg/ml leupeptin, 1 mM Na_3VO_4, and 1 mM PMSF. For PI3 kinase assay, immune complexes were analyzed as described below. For gel electrophoresis and immunoblotting, immune complexes were solubilized in 2× concentrated SDS-containing sample buffer, separated by SDS-PAGE, and electrophoretically transferred to Immobilon-P membrane (Millipore Corp., Bedford, MA). Immunoreactive proteins were detected by ECL as above.

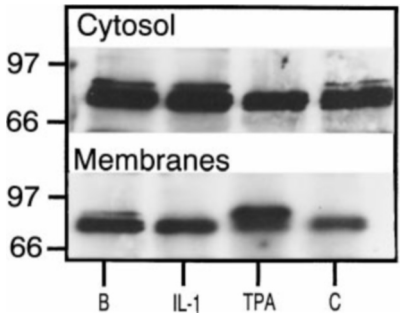

FIG. 1. **BCP crystal induction of PKC translocation.** Confluent, quiescent HF cultures in DMEM and 0.5% FBS were treated with BCP crystals (18 $\mu g/cm^2$). Control cultures were treated with IL-1 (50 ng/ml), TPA (200 nM), or left untreated. After 20 min, cultures were harvested, and cytosolic and membrane fractions were prepared as described under "Experimental Procedures." Western blot of cytosolic and membrane fractions of HF using a monoclonal anti-PKC antibody (MC-5) was performed. *B,* BCP crystals; *C,* control, unstimulated cultures. The positions of molecular mass markers in kDa are shown.

Phosphatidylinositol 3-Kinase Assay—Washed anti-PI3K immunoprecipitates were incubated on ice for 10 min in 20 μl of a sonicated substrate mixture containing PtdIns(4,5)P_2 and phosphatidylserine (1:1) at a concentration of 0.5 mg/ml in 20 mM HEPES, pH 7.4. Reactions were initiated by addition of 20 μl of kinase buffer containing 20 mM HEPES, pH 7.4, 50 mM $MgCl_2$, 50 μM ATP, 20 μCi of [γ-^{32}P]ATP (specific activity, 6000 Ci/mmol; NEN Life Science Products). After 10 min at 37 °C, the reactions were terminated with 200 μl of 1 N HCl. Next, $CHCl_3/CH_3OH$ (1:1) (400 μl) was added, and the phospholipids were extracted. The aqueous layer was aspirated, and the $CHCl_3$ layer was washed once with 160 μl of CH_3OH/1 N HCl (1:1). The resulting $CHCl_3$ layer was dried with nitrogen gas, and the phospholipid residues were solubilized in $CHCl_3/CH_3OH$ (2:1). Radiolabeled PtdIns(3,4,5)P_3 was separated from PtdIns(4,5)P_2 and PtdIns(4)P standards by thin layer chromatography (TLC) as described previously (39). ^{32}P-Radiolabeled phosphoinositides were visualized by autoradiography. $^{32}P_i$ incorporated into PtdIns(3,4,5)P_3 was quantified directly on the TLC plates with an AMBIS computerized imaging/radioscanning system. Authentic PtdIns(4)P and PtdIns(4,5)P_2 standards were chromatographed in parallel lanes and visualized by spraying with 10% H_2SO_4 and heating to 100 °C.

Statistics

Statistical analysis was performed using the Wilcoxon Rank Sum test (40).

RESULTS

BCP Crystals Cause PKC Translocation—PKC activation is associated with translocation of the enzyme from the cytosolic to the membrane fraction of the cell. The addition of BCP crystals (18 $\mu g/cm^2$) or TPA (200 nM) to HF cultures in 0.5% FBS/DMEM caused translocation of an upper band, immunoreactive with the monoclonal anti-PKC antibody (clone MC5), from the cytosolic compartment to the membrane compartment of HF harvested 15 min after treatment (Fig. 1). Treatment of HF with IL-1 (50 ng/ml) showed no such effect. Translocation of the immunoreactive band was maximal when cells were harvested 10 min after treatment with BCP crystals and returned to control levels within 30 min after stimulation (Fig. 2).

Inhibition of BCP Crystal-induced HF Mitogenesis by the PKC Inhibitor Staurosporine—By using [^{3}H]thymidine incorporation as an index of mitogenesis, we demonstrated a 5-fold increase in [^{3}H]thymidine incorporation in HF cultures treated with BCP crystals (25 $\mu g/cm^2$) compared with that of control HF cultures incubated with 0.5% FBS alone after 24 h (Fig. 3). Staurosporine, which inhibits PKC by interacting with the catalytic domain, attenuated the mitogenic response of HF to BCP crystals in a concentration-dependent fashion. Similarly, the phorbol ester TPA (200 nM), a known activator of PKC, caused a 2½-fold increase in [^{3}H]thymidine incorporation in HF cultures. Staurosporine inhibited the mitogenic response to

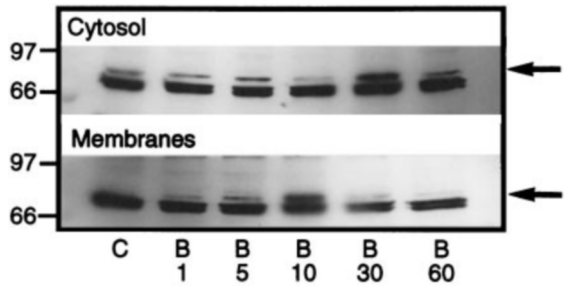

FIG. 2. **BCP crystal induction of PKC translocation, time course**. Confluent, quiescent HF cultures in DMEM and 0.5% FBS were treated with BCP crystal (18 $\mu g/cm^2$). Control cultures were in DMEM and 0.5% FBS. At the indicated time points in minutes, cultures were harvested, and cytosolic and membrane fractions were prepared as described under "Experimental Procedures." Western blot of cytosolic and membrane fractions of HF using a monoclonal anti-PKC antibody (MC-5) was performed. *C,* control, unstimulated cultures; *B,* BCP crystals. The positions of molecular mass markers in kDa are shown.

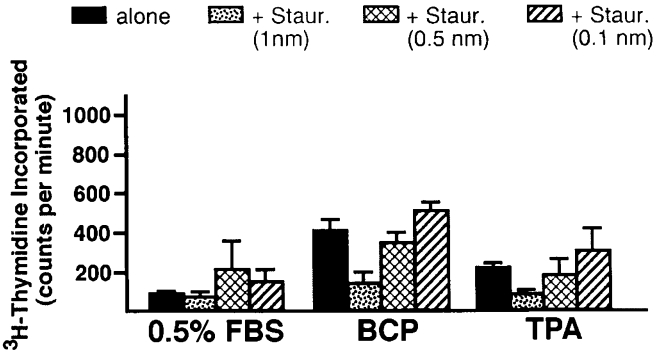

FIG. 3. **Effect of the PKC inhibitor, staurosporine, on BCP crystal-induced mitogenesis.** Confluent, quiescent HF cultures in DMEM and 0.5% FBS were treated with BCP crystals (25 $\mu g/cm^2$) with or without staurosporine at varying doses. Staurosporine was added 30 min prior to other stimulants. Control cultures were treated with the phorbol ester, TPA (200 nM), or 10% serum, or were unstimulated. After 23 h, all plates were pulse-labeled with [^{3}H]thymidine (1 μCi/ml) for 1 h. The plates were then processed, and thymidine incorporation was determined. All values ± S.E.; $n = 6$. *Staur,* staurosporine. Significant inhibition of BCP crystal- and TPA-induced mitogenesis by staurosporine (1 nM), $p < 0.01$.

TPA in a concentration-dependent manner. When HF were incubated with staurosporine alone, there was a modest increase in [^{3}H]thymidine incorporation at 0.5 and 0.1 nM concentrations.

BCP Crystals Cause Increased PKC Activity—The addition of BCP crystals (25 $\mu g/cm^2$) to HF cultures in 0.5% FBS/DMEM produced an approximately 3-fold increase in PKC activity after 30 min (Table I). TPA (200 nM) caused an approximately 5-fold increase in PKC activity after 30 min. The increases in PKC activity induced by both BCP crystals and TPA were attenuated by the PKC inhibitors staurosporine, bisindolylmaleimide-1 (a competitive inhibitor for the ATP-binding site of PKC), and H7. To preclude inhibition of a cAMP-dependent kinase, we also investigated the effects of HA1004, a compound structurally similar to H7 but with a higher K_i for PKC (K_i PKC, 40 μM; K_i, cAMP-dependent kinase 2.3 μM) (37). HA1004 had no inhibitory effect on BCP- or TPA-induced increases in PKC activity.

BCP Crystals Induce NF-κB in Balb/c/3T3 Fibroblasts—By using the UV21 probe, BCP crystal-induced NF-κB was demonstrated in Balb/c/3T3 fibroblasts by formation of an NF-κB·DNA complex within 30 min of treatment which was maximal within 60 min of treatment and which had returned to base line by 24 h after treatment (Fig. 4). When nuclear extracts were treated with recombinant IκB prior to addition of

TABLE I
BCP crystal induction of PKC activity in human fibroblasts, effect of PKC inhibitors

HF cultures were treated with various agents. At 30 min, cultures were harvested and membrane PKC activity was determined after elution from DEAE columns as described under "Experimental Procedures." $n = 4 \pm$ S.E. Concentration of BCP crystals, 25 $\mu g/cm^2$; TPA, 10 nM; staurosporine, 10 nM; bisindolylmaleimide-1, 10 nM; H7, 10 μM; HA1004, 10 μM.

Addition	Control	BCP	TPA
No addition	9.1 ± 1.2	31.8 ± 2.8	50.1 ± 6
Staurosporine	10.0 ± 0.2	11.9 ± 0.9	12.5 ± 0.3
H7	11.3 ± 1.8	14.9 ± 0.9	16.8 ± 3.2
HA1004	8.7 ± 1.4	34.5 ± 6.3	58.4 ± 7.8
Bisindolymaleimide-1	7.4 ± 1.6	13.1 ± 2.0	17.0 ± 2.1

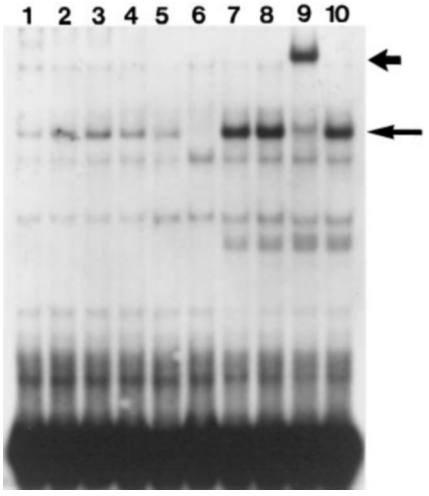

FIG. 4. **BCP crystal induction of NF-κB in Balb/c/3T3 fibroblasts.** EMSA of equal amounts of protein from nuclear extracts of untreated or BCP crystal-stimulated Balb/c/3T3 fibroblasts was performed using the probe described under "Experimental Procedures." *Lane 1*, unstimulated cell extracts; *lanes 2–5,* time course of induction of NF-κB. *Lane 2,* 30 min; *lane 3,* 60 min; *lane 4,* 90 min; *lane 5,* 24 h after treatment with BCP crystals. *Lane 6*, BCP crystal-stimulated cell extracts co-incubated with IκB. *Lane 7*, BCP crystal-stimulated cell extracts co-incubated with antibody 1141 against p50. *Lane 8*, BCP crystal-stimulated cell extracts co-incubated with antibody 1141 and its corresponding peptide. *Lane 9*, BCP crystal-stimulated cell extracts co-incubated with antibody 5192 against p65. *Lane 10*, BCP crystal-stimulated cell extracts co-incubated with antibody 5192 and its corresponding peptide. The *thin arrow* indicates the major complex induced and the *thick arrow* indicates the supershifted complex.

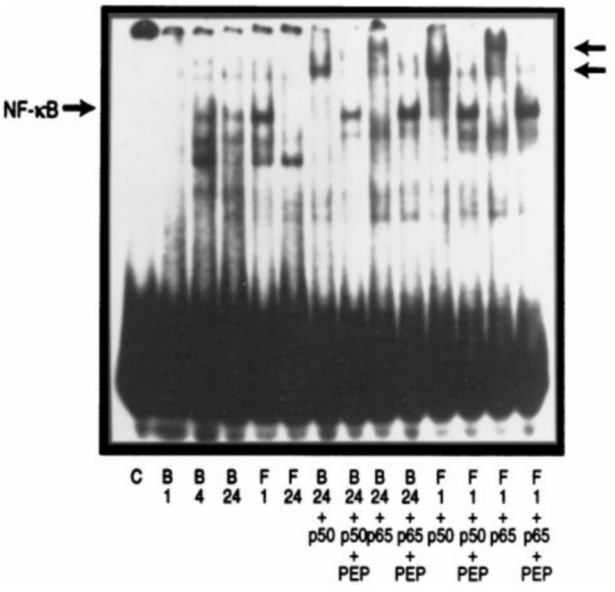

FIG. 5. **BCP crystal induction of NF-κB in HF, time course.** EMSA of equal amounts of protein from nuclear extracts of untreated, BCP crystal-stimulated, or 10% FBS-treated HF was performed using the probe described under "Experimental Procedures." Cells were harvested at the indicated times in hours after stimulation. *C,* unstimulated control cultures; *B,* BCP (18 $\mu g/cm^2$) crystal-stimulated cultures; *F,* 10% FBS-treated cultures; numbers refer to time in hours after treatment. *p50,* polyclonal anti-peptide antibody to p50 (antibody 1141); *p65,* polyclonal anti-peptide antibody against p65; *pep,* corresponding peptide. *Unlabeled arrows* show the position of the supershifted complexes.

the UV21 probe, DNA binding of the protein complex was completely inhibited. Co-incubation of the nuclear extracts with an anti-p65 antibody caused a supershift of the NF-κB·DNA complex, confirming the specificity of binding. The addition of an anti-p50 antibody did not result in a supershifted NF-κB·DNA complex, likely due to inability of the human antibody to recognize murine protein.

BCP Crystals Cause NF-κB Induction in HF—BCP crystal-induced NF-κB was demonstrated in HF by formation of an NF-κB·DNA complex within 4 h of treatment which continued through 24 h after treatment, the longest time point tested (Fig. 5). Co-incubation of the nuclear extracts with either an anti-p65 or anti-p50 antibody resulted in a supershifted complex. The induction of NF-κB by BCP crystals was delayed relative to the induction of NF-κB in response to 10% FBS as treatment of cultures with 10% FBS resulted in formation of an NF-κB·DNA complex within 1 h which had returned to base line within 24 h after treatment. Control cultures were in 0.5% FBS.

When BCP crystal-treated HF cultures were co-incubated with the PKC inhibitor staurosporine, there was a concentration-dependent inhibition of BCP crystal-induced NF-κB. Such inhibition was not specific as NF-κB induction in response to 10% FBS was also inhibited (Fig. 6). Concurrent with BCP crystal induction of NF-κB, there was transient disappearance of immunoreactive I-κBa noted both 1 and 4 h after treatment with BCP crystals. There was reappearance of I-κB by 24 h after treatment (Fig. 7).

BCP Crystals Induce c-fos and c-jun mRNA and AP-1 in HF—BCP crystals caused maximal expression of c-*fos* mRNA in HF 30 min after treatment which returned to base line within 2 h (Fig. 8, *A* and *B*). When cultures were treated with staurosporine prior to stimulation with BCP crystals, c-*fos* mRNA expression was greatly attenuated. BCP crystals induced maximal expression of c-*jun* mRNA within 2 h after treatment which continued through 3 h, the longest time point tested (Fig. 8, *C* and *D*). In contrast with c-*fos*, there was minimal inhibition of c-*jun* mRNA when cultures were treated with staurosporine. Complementing these findings, BCP crystals induced nuclear translocation of the transcription factor AP-1 which continued for at least 2 h after treatment, the longest time point tested (Fig. 9, *A* and *B*). Nuclear binding was specific as none resulted from incubation with a mutant AP-1 probe. Control HF cultures were in 0.5% FBS, 10% FBS, or treated with TPA (200 nM). Co-incubation of the nuclear extracts with an anti-Fos antibody resulted in a supershifted complex.

BCP Crystals Do Not Induce Protein Tyrosine Phosphorylation or Activation of PI3 Kinase—Base-line levels of four tyrosine-phosphorylated proteins were observed in lysates from control and, unstimulated cultures. Bands at 50 and 27 kDa correspond to heavy and light chain antibody, respectively, reacting with secondary HRP-conjugated goat anti-mouse IgG. When cultures were treated with PDGF (50 ng/ml), there was enhanced tyrosine phosphorylation of a number of proteins with molecular masses of 185, 170, 145, 116, 80, 72, 62, 60, 40,

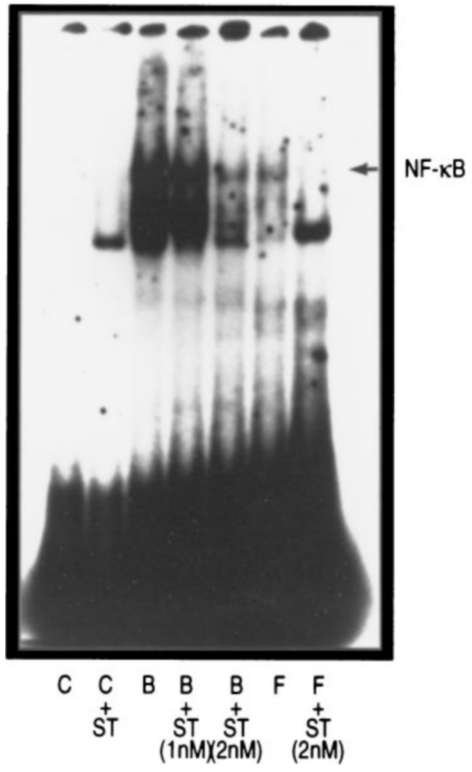

FIG. 6. **BCP crystal induction of NF-κB in HF.** Effect of the PKC inhibitor, staurosporine. EMSA of equal amounts of protein from nuclear extracts of untreated, BCP crystal-stimulated or 10% FBS-treated HF was performed using the probe described under "Experimental Procedures." *C,* unstimulated control cultures; *ST,* staurosporine (1 nM); *B,* BCP (18 $\mu g/cm^2$) crystal-stimulated cultures; *F,* 10% FBS-treated cultures.

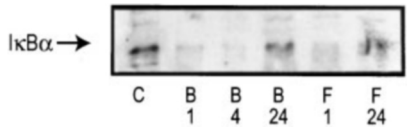

FIG. 7. **BCP crystal induction of transient disappearance of IκB in HF**. Cytoplasmic extracts (50 μg) were subjected to PAGE followed by Western blot using a polyclonal antibody to IkBα (1:1000). *C,* untreated control cultures; *B,* BCP crystals; *F,* 0% FBS. *Numbers* refer to time in hours after treatment when cultures were harvested.

and 33 kDa. In contrast, cells treated with either BCP crystals or the non-mitogenic particulate controls, latex beads or diamond dust, resulted in no increase in tyrosine phosphorylation relative to unstimulated cultures (Fig. 10*A*). Similarly, when HF cultures were treated with PDGF and lysates immunoprecipitated with anti-phosphotyrosine antibody, as expected, PI3 kinase activity on the immune complexes was dramatically increased over unstimulated cells (Fig. 10*B, lane 3 versus 4*). However, PI3 kinase activity on anti-phosphotyrosine immune complexes from BCP-treated cells was no different from untreated cells (*lane 3 versus 5*). NIH 3T3 cells treated with PDGF and immunoprecipitated with either phosphotyrosine or anti-PI3 kinase antibodies served as positive controls (*lanes 1* and *2*). Untreated, PDGF-treated, or BCP-treated HF cells immunoprecipitated with PI3 kinase antibody also served as positive controls for PI3 kinase activity (*lanes 6–8*).

DISCUSSION

The results of this investigation show that BCP crystal-induced cell activation is associated with NF-κB induction in Balb/c/3T3 and human fibroblasts (HF) and PKC activation and AP-1 induction in HF. Moreover, we have demonstrated that inhibition of BCP crystal-induced mitogenesis by the PKC inhibitor staurosporine is accompanied by inhibition of BCP crystal induction of NF-κB and c-*fos*, but not c-*jun*, mRNA. Although the cellular effects of many other growth-promoting agents are mediated by high affinity receptor protein tyrosine kinases (PTK) (14) with resultant recruitment and activation of PI3K (15), out data show that neither tyrosine phosphorylation nor PI3K activity appears to be required for BCP crystal-induced cell activation. Thus, these observations further define the biological effects of BCP crystals.

BCP crystals cause mitogenesis in Balb/c/3T3 murine fibroblasts, and NF-κB is induced when quiescent Balb/c/3T3 fibroblasts are stimulated with serum growth factors (6, 11). Therefore, we initiated our investigation by studying the ability of BCP crystals to induce NF-κB in this cell type. We were unable to demonstrate the presence of the p50 subunit in the NF-κB·DNA complex by supershift in Balb/c/3T3 cells treated with BCP crystals. However, the antibody was raised against a peptide fragment from human, and not murine, p105, the cytoplasmic precursor of p50 and therefore may not recognize murine protein.

BCP crystals possess many of the characteristics typical of a growth factor. Most water-soluble hormones or growth factors bind to specific receptors on the cell surface which induce the intracellular activation of signaling cascades. The mediator of the earliest events induced by contact of insoluble BCP crystals with the cell surface, or with an as yet unknown surface "receptor," has not yet been identified. We have used PDGF as a control in our work because the PDGF receptor has been characterized, and the signal transduction pathways induced by the PDGF receptor have been analyzed in detail (41). In contrast to that of BCP crystals, PTK and PI3 kinase are required for PDGF-induced DNA synthesis (16). Furthermore, PDGF-induced DNA synthesis occurs through a protein kinase C (PKC)-independent pathway, whereas BCP crystals require at least basal levels of PKC to induce mitogenesis (6).

PTK and PI3K are involved in CPPD crystal-induced neutrophil activation (17, 18). Although both are calcium-containing, CPPD and BCP crystals differ in their clinical manifestations. CPPD is commonly associated with attacks of acute arthritis, "pseudogout," characterized by joint effusions packed with neutrophils. BCP crystals in synovial fluid, in contrast, are usually associated with few neutrophils. It is not known whether BCP crystals induce PTK or PI3K in neutrophils. BCP crystals did not induce PTK or PI3K in human fibroblasts, in contrast with PDGF (6). These results emphasize the specificity of cell activation by BCP crystals and suggest that BCP crystals, unlike PDGF, directly or indirectly activate G-protein-linked surface receptor(s) (42).

Many stimuli other than BCP crystals activate NF-κB. These include cytokines and activators of protein kinase C such as the phorbol ester TPA (43). Several signal transduction pathways may be involved, but all of these stimuli act by means of protein kinases that phosphorylate (and thus degrade) IκB. It was originally proposed that IκB might serve as a substrate for kinases such as PKC and protein kinase A, based on *in vitro* studies (44, 45). Recently, however, a high molecular mass IκB kinase complex containing at least two cytokine-responsive IkB kinases has been identified (46). These kinases specifically phosphorylate critical serine residues of IκB. Activation of NF-κB by tumor necrosis factor-α and IL-1 requires the successive action of NF-κB-inducing kinase and IκB kinase (47). The molecular mechanisms by which NF-κB-inducing kinase becomes activated are not yet understood. Although BCP crystals activate both PKC and NF-κB, it is not known to what extent these two events are linked. Since the critical modification for IkB kinases activation appears to be phosphorylation,

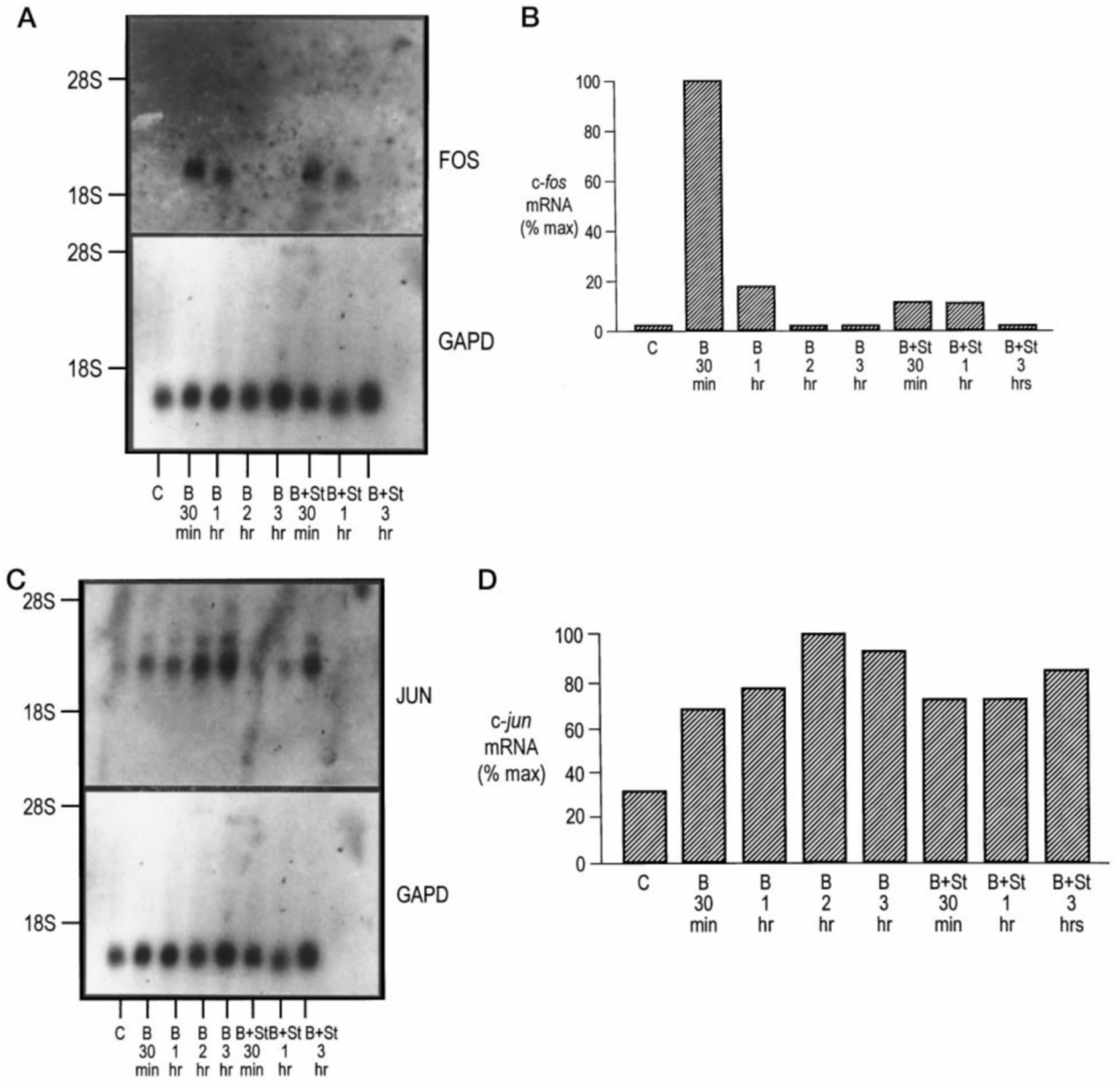

FIG. 8. **BCP crystal induction of c-*fos* (*A* and *B*) and c-*jun* (*C* and *D*) mRNA accumulation, effect of staurosporine.** Confluent cultures of HF in 100-mm plates were incubated in DMEM and 0.5% FBS for 24 h before being treated with BCP crystals (18 $\mu g/cm^2$). Some cultures were treated with staurosporine (1 nM) 30 min prior to stimulation with BCP crystals. Unstimulated control cultures were in 0.5% FBS. At varying time points, cultures were harvested, and total RNA was isolated. Northern blot analysis was performed using radiolabeled c-*fos* cDNA, followed by autoradiography. The blot was then stripped of the c-*fos* probe and re-probed with radiolabeled c-*jun* cDNA, and autoradiography repeated. The blot was stripped one more time and re-probed with radiolabeled glyceraldehyde-3-phosphate dehydrogenase (*GAPD*) cDNA as a control. Autoradiographs were scanned using a laser densitometer with results presented as *bar graphs* and expressed as the percent of maximal expression, using glyceraldehyde-3-phosphate dehydrogenase to correct for small variations in total RNA analyzed. *B,* BCP crystals; *St,* staurosporine. The positions of the 18 S and 28 S ribosomes are shown.

it is possible that PKC plays a role in BCP crystal induction of NF-κB by inducing phosphorylation and activation of IkB kinases (48). In support of this concept, the PKC inhibitor staurosporine inhibited both BCP crystal-induced mitogenesis and NF-κB. Alternatively, it is possible that staurosporine inhibits IkB kinases since, although it is a potent inhibitor of PKC, it also inhibits PKA and other protein kinases (49).

BCP crystals induce MMP synthesis and secretion in fibroblasts and chondrocytes, but the mechanism by which this occurs remains poorly understood. We have shown that while intracellular dissolution of BCP crystals augments the mitogenic response, it does not play a role in BCP induction of MMPs (50). The mechanism of stimulation of the synthesis and secretion of MMPs in response to stimuli other than BCP crystals is partly understood. For example, PKC activation is required for MMP induction in fibroblasts treated with epidermal growth factor (51) or interleukin-1 (52). Although PKC activation occurs with BCP crystal-induced mitogenesis, its role in the associated MMP production has not been established. Staurosporine does not inhibit BCP crystal-induced collagenase mRNA accumulation in HF[2] at concentrations which inhibit mitogenesis. We have shown here that staurosporine inhibited BCP crystal-induced c-*fos* but not c-*jun* mRNA accumulation in HF. This suggests that BCP crystal-induction of c-*fos* requires PKC activity, whereas induction of c-*jun* does

[2] G. M. McCarthy, unpublished observations.

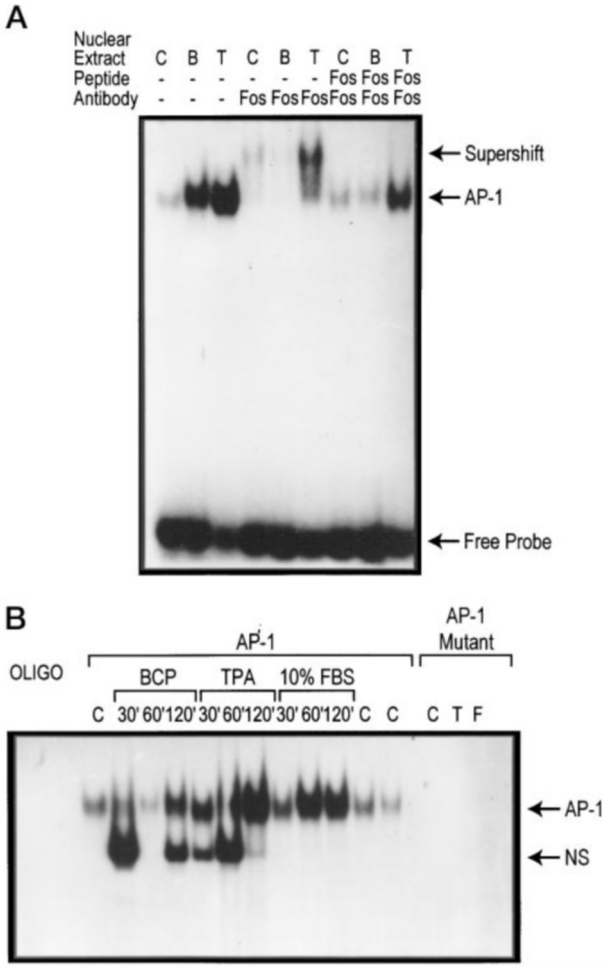

FIG. 9. **BCP crystal induction of AP-1**. *A,* EMSA of equal amounts of protein from nuclear extracts of HF treated with BCP crystals (18 $\mu g/cm^2$) was performed using the radiolabeled AP-1 probe, as described under "Experimental Procedures." Control cultures were treated with TPA (200 nM) or left untreated. Cultures were harvested 2 h after treatment. Some extracts were co-incubated with a polyclonal anti-Fos antibody with or without its corresponding peptide. The positions of AP-1 and the supershifted complexes are shown. *C,* unstimulated cultures; *B,* BCP crystal-treated cultures; *T,* TPA-treated cultures. *B,* time course. EMSA was performed as above, but some extracts were incubated with the mutant AP-1 probe described under "Experimental Procedures." Control cultures were untreated or treated with TPA (200 nM) or 10% FBS. *C,* unstimulated cultures; *T,* TPA; *F,* 10% FBS. *Numbers* refer to time in min (′) after treatment when cultures were harvested. *NS,* nonspecific.

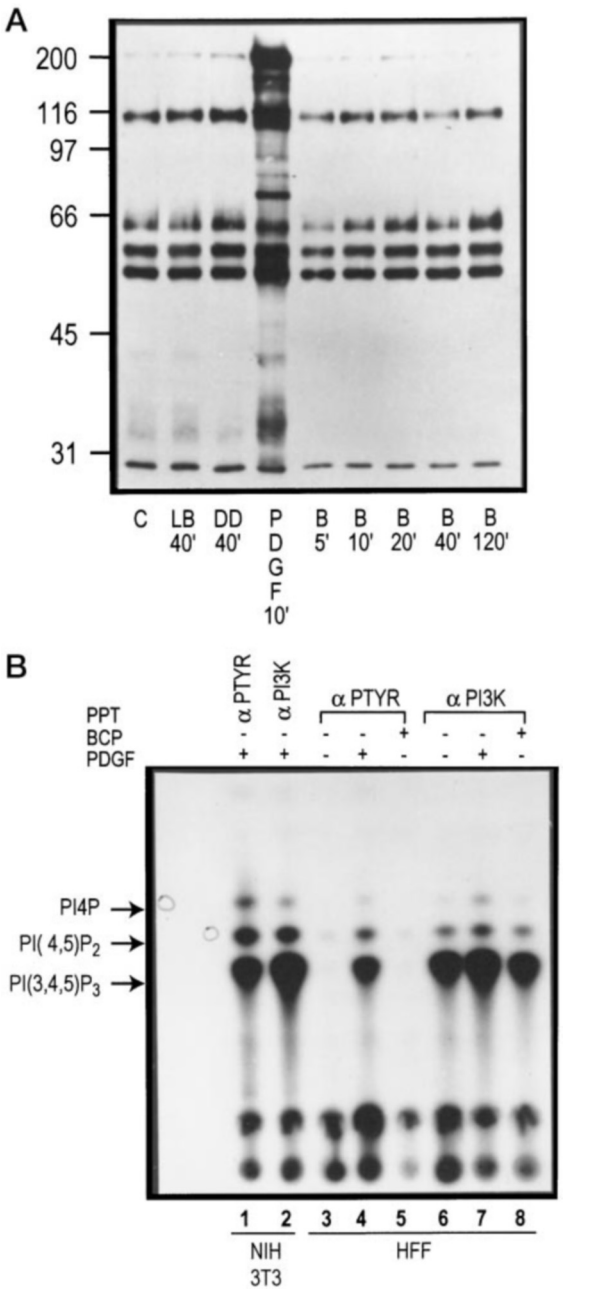

FIG. 10. **PDGF- or BCP crystal-induced protein tyrosine phosphorylation and phosphatidylinositol 3-kinase activation in fibroblasts.** *A,* confluent HF in 100-mm plates were incubated overnight in 0.5% FBS and either left untreated (*C*) or treated with latex beads (18 $\mu g/cm^2$), diamond dust (18 $\mu g/cm^2$), BCP crystals (18 $\mu g/cm^2$), or PDGF (50 ng/ml) for the times (′, min) indicated. Cell lysates were immunoprecipitated with anti-phosphotyrosine antibody 4G10 as described under "Experimental Procedures." Immune complexes were solubilized in SDS sample buffer, separated by 8.75% SDS-PAGE, and immunoblotted with 4G10 antibody as described under "Experimental Procedures." Tyrosine-phosphorylated proteins were detected by chemiluminescence. Molecular mass markers in kDa are indicated at the *left*. *B,* NIH 3T3 or human fibroblasts were either untreated (*C*) or treated as in *A* with either BCP crystals (18 $\mu g/cm^2$) or PDGF (50 ng/ml) for 15 min. Cell lysates were immunoprecipitated (*PPT*) with either anti-phosphotyrosine antibody 4G10 or anti-PI3K antibody as described under "Experimental Procedures." The PI3K assay, as described under "Experimental Procedures," was used to assess PI3K activity on the washed immune complexes using PtdIns(4,5)P_2 as substrate. Lipids were separated by thin layer chromatography and radiolabeled PtdIns(3,4,5)P_3 was detected by autoradiography. Net counts incorporated into PtdIns(3,4,5)P_3 are as follows: *lane 1*, 9,120; *lane 2,* 41,741; *lane 3*, 108; *lane 4*, 4,581; *lane 5*, 22; *lane 6*, 13,092; *lane 7*, 30,214; and *lane 8*, 10,038. *Circles* represent migration of authentic PtdIns(4)P and PtdIns(4,5)P_2 standards.

not. Members of the AP-1 family of transcription factors include Fos/Jun or Jun/Jun dimers that bind preferentially to the TRE of the collagenase promotor (53). It is possible that the lack of inhibition of BCP crystal-induced c-*jun* or collagenase mRNA accumulation in the presence of staurosporine reflects binding of Jun/Jun dimers to the TRE during BCP crystal induction of MMP1 and other MMPs. Alternatively, since MAP kinases also modulate AP-1 activity (53), BCP crystal-induced activation of MAP kinases could facilitate MMP production in the presence of staurosporine (8).

The AP-1 sequence or TRE is necessary but not sufficient for phorbol ester induction of collagenase in fibroblasts (54). Furthermore, in some cells MMP expression is dependent on activation of and DNA binding to NF-κB but not AP-1 (55). Conversely, the functional and physical interplay of the NF-κB and AP-1 families of transcription factors have recently been reported to result in enhanced DNA binding and biological function of each (56). Finally, the potential role of the transcription

factor PEA3 in the transcriptional regulation of BCP crystal-induced MMP expression needs to be considered as the collagenase promotor contains a PEA3-binding site that acts synergistically with AP-1 to achieve maximal levels of transcriptional activation in response to TPA (57). BCP crystals induce both NF-κB and AP-1, and our data suggest that NF-κB plays a role in BCP crystal-induced mitogenesis and that AP-1 is involved in BCP crystal induction of MMPs. Further study will be necessary to show whether NF-κB and/or PEA3 activation is necessary for BCP crystal induction of MMPs.

Glucocorticoids are potent inhibitors of NF-κB activation in mice and cultured cells. Such inhibition appears to be mediated by induction of IκBα inhibitory protein (58). Glucocorticoids also inhibit MMP-1 induction by interfering with AP-1 (59–61). Intra-articular glucocorticoids are effective for at least short-term relief of pain in OA, but no clinical predictors of response have been found (62). The presence or absence of synovial fluid BCP crystals was not evaluated, however, and based on the current data, glucocorticoids likely inhibit the major biological effects of BCP crystals *in vivo*. In addition, aspirin and sodium salicylate, both of which have been used to treat the symptoms of joint degeneration, also inhibit the activation of NF-κB so that the anti-inflammatory effects of these drugs may be partly attributable to the inhibition of NF-κB (63). Finally, a number of PKC modulators are currently undergoing clinical evaluation as anticancer drugs, and tamoxifen, already in clinical use, is a moderately potent inhibitor of PKC (64). PKC inhibition could be an effective target for attenuation of BCP crystal-induced mitogenesis.

The association of BCP crystals with osteoarthritis and joint destruction is well established. Synovial hypertrophy is likely a response to the mitogenic effects of the crystals, and degradation of cartilage likely results from MMP activity induced by the crystals in synoviocytes and chondrocytes. However, no known drug prevents or treats the consequences of BCP crystal deposition. An improved understanding of the molecular mechanisms leading to BCP crystal-induced mitogenesis and MMP induction is essential to the development of a rational approach to ultimate prevention or reversal of the consequences of BCP crystal deposition.

REFERENCES

1. Halverson, P. B. and McCarty, D. J. (1997) in *Arthritis and Allied Conditions: A Textbook of Rheumatology* (Koopman, W. J., ed) pp. 2127–2146, Williams & Wilkins, Baltimore
2. Halverson, P. B., and McCarty, D. J. (1986) *Ann. Rheum. Dis*. **45,** 603–605
3. Carroll, G. J., Stuart, R. A., Armstrong, J. A., Breidahl, P. D., and Laing, B. A. (1991) *J. Rheumatol.* **18,** 861–866
4. McCarty, D. J., Halverson, P. B., Carrera, G. F., Brewer, B. J., and Kozin, F. K. (1981) *Arthritis & Rheum.* **24,** 464–473
5. Cheung, H. S., Story, M. T., and McCarty, D. J. (1984) *Arthritis & Rheum.* **27,** 668–674
6. Mitchell, P. G., Pledger, W. J., and Cheung, H. S. (1989) *J. Biol. Chem.* **264,** 14071–14077
7. Cheung, H. S., and McCarty, D. J. (1985) *Exp. Cell Res.* **157,** 63–70
8. Nair, D., Misra, R. P., Sallis, J. D., and Cheung, H. S. (1997) *J. Biol. Chem.* **272,** 18920–18925
9. Rothenberg, R., and Cheung, H. (1988) *Am. J. Physiol*. **254,** C554–C559
10. Mitchell, P. G., Struve, J. A., McCarthy, G. M., and Cheung, H. S. (1992) *Arthritis & Rheum.* **35,** 343–350
11. Baldwin, A., Clifford Azizkahn, J., Jensen, D., Beg, A., and Coodly, L. (1991) *Mol. Cell. Biol*. **11,** 4943–4951
12. Baldwin, A. S. (1996) *Annu. Rev. Immunol*. **14,** 649–681
13. Chen, Z. J., Parent, L., and Maniatis, T. (1996) *Cell* **84,** 853–862
14. Fantl, W. J., Johnson, D. E., and Williams, L. T. (1993) *Annu. Rev. Biochem.* **62,** 453–481
15. Kapeller, R., and Cantley, L. C. (1994) *BioEssays* **16,** 565–576
16. Roche, S., Koegl, M., and Courtneidge, S. (1994) *Proc. Natl. Acad. Sci. U. S. A.* **91,** 9185–9189
17. Gaudry, M., Roberge, C. J., de Medicis, R., Lussier, A., Poubelle, P. E., and Naccache, P. H. (1993) *J. Clin. Invest.* **91,** 1649–1655
18. Jackson, J. K., Lauener, R., Duronio, V., and Burt, H. M. (1997) *J. Rheumatol.* **24,** 341–348
19. McCarthy, G. M., Mitchell, P. G., Struve, J. S., and Cheung, H. S. (1992) *J. Cell. Physiol*. **153,** 140–146
20. McCarthy, G., Macius, A., Christopherson, P., Ryan, L., and Pourmotabbed, T. (1998) *Ann. Rheum. Dis*. **57,** 56–60
21. McCarthy, G., Christopherson, P., and Mitchell, P. (1997) *Arthritis & Rheum.* **40,** 127 (abstr.)
22. Brenner, D., O'Hara, M., Angel, P., Chojkier, M., and Karin, M. (1989) *Nature* **337,** 661–663
23. Angel, P., Baumann, I., Stein, B., Delius, H., Rahmsdorf, H., and Herrich, P. (1987) *Mol. Cell. Biol.* **7,** 2256–2266
24. Cheung, H., Sallis, J., and Struve, J. (1996) *Biochim. Biophys. Acta* **1315,** 105–111
25. Curran, T., Peters, G., van Beveren, C., Teich, N., and Verma, I. (1982) *J. Virol.* **44,** 674–682
26. Angel, P., Allegretto, E., Okino, S., Hattori, K., Boyle, W., Hunter, T., and Karin, M. (1988) *Nature* **332,** 166–171
27. Tso, J. Y., Sun, X. H., Kao, T. H., Reece, K. S., and Wu, R. (1985) *Nucleic Acids Res.* **13,** 2485–2502
28. McCarthy, G. M., Mitchell, P. G., and Cheung, H. S. (1991) *Arthritis & Rheum*. **34,** 1021–1030
29. Evans, R. W., Cheung, H. S., and McCarty, D. J. (1984) *Calcif. Tissue Int*. **36,** 645–650
30. Laemmli, U. K. (1970) *Nature* **227,** 680–685
31. Bradford, M. (1976) *Anal. Biochem.* **72,** 248–254
32. Scheinmann, R. I., Beg, A., and Baldwin, A. (1993) *Mol. Cell. Biol.* **13,** 6089–6101
33. Cathala, G., Savouret, J., Mendez, B., West, B. L., Karin, M., Martial, J. A., and Baxter, J. D. (1983) *DNA* (*N. Y.*) **2,** 329–335
34. Davis, L. G., Dibner, M. D., and Battey, J. F. (1986) in *Basic Methods in Molecular Biology,* pp. 143–146, Elsevier Science Publishing Co., Inc., New York
35. Feinberg, A. P., and Vogelstein, B. (1983) *Anal. Biochem*. **132,** 6–9
36. Gusovsky, F., and Gutkind, J. S. (1991) *Mol. Pharmacol.* **39,** 124–129
37. Mitchell, P., and Cheung, H. (1993) *Biochem. Biophys. Res. Commun.* **196,** 1133–1142
38. Hannun, Y., Loomis, C., and Bell, R. (1985) *J. Biol. Chem.* **260,** 10039–10043
39. Augustine, J. A., Sutor, S. L., and Abraham, R. T. (1991) *Mol. Cell. Biol*. **11,** 4431–4440
40. Rimm, A. A., Hartz, A. J., Kalbfleisch, J. H., Anderson, A. J., and Hoffmann, R. G. (1980) *Basic Biostatistics in Medicine and Epidemiology,* pp. 267–281, Appleton-Century-Crofts, New York
41. Alberts, B., Bray, D., Lewis, J., Raff, M., Roberts, K., and Watson, J. (1994) *Molecular Biology of the Cell,* pp. 721–778, Garland Publishing, Inc., New York
42. Sternweis, P. C., and Smrcka, A. V. (1992) *Trends Biochem. Sci.* **17,** 502–506
43. Barnes, P. and Karin, M. (1997) *N. Engl. J. Med.* **336,** 1066–1071
44. Baeuerle, P. A., and Baltimore, D. (1988) *Science* **242,** 540–546
45. Shirakawa, F., and Mizel, S. B. (1989) *Mol. Cell. Biol.* **9,** 2424–2430
46. Mercurio, F., Zhu, H., Murray, B. W., Shevchenko, A., Bennett, B. L., Li, J., Young, D. B., Barbosa, M., Mann, M., Manning, A. and Rao, A. (1997) *Science* **278,** 860–866
47. Woronicz, J. D., Gao, X., Cao, Z., Rothe, M., and Goeddel, D. V. (1997) *Science* **278,** 866–869
48. DiDonato, J. A., Hayakawa, M., Rothwarf, D. M., Zandi, E., and Karin, M. (1997) *Nature* **388,** 548–554
49. Tamaoki, T. (1991) *Methods Enzymol.* **201,** 340–347
50. McCarthy, G. M., Cheung, H. S., Abel, S. M., and Ryan, L. M. (1998) *Osteoarthritis Cartilage* **6,** 205–213
51. McDonnell, S. E., Kerr, L. D., and Matrisian, L. M. (1990) *Mol. Cell. Biol*. **10,** 4284–4293
52. Case, J. P., Lafyatis, R., Kumkumian, G. K., Remmers, E. F., and Wilder, R. L. (1990) *J. Immunol.* **145,** 3755–3761
53. Karin, M., Liu, Z., and Zandi, E. (1997) *Curr. Opin. Cell Biol.* **9,** 240–246
54. Auble, D., and Brinckerhoff, C. (1991) *Biochemistry* **30,** 4629–4635
55. Zhang, B., Geng, Y., and Lotz, M. (1992) *Arthritis & Rheum.* **35,** 49 (abstr.)
56. Stein, B., Baldwin, A., Ballard, D., Greene, W., Angel, P., and Herrlich, P. (1993) *EMBO J*. **12,** 3879–3891
57. Gutman, A., and Wasylyk, B. (1990) *EMBO J*. **9,** 2241–2246
58. Scheinman, R. I., Cogswell, P. C., Lofquist, A. K., and Baldwin, A. S., Jr. (1995) *Science* **270,** 283–286
59. Jonat, C., Rahmsdorf, H. J., Park, K. K., Cato, A. C., Gebel, S., Ponta, H., and Herrlich, P. (1990) *Cell* **62,** 1189–1204
60. Lucibello, F. C., Slater, E. P., Jooss, K. U., Beatu, M., and Muller, R. (1990) *EMBO J.* **9,** 2827–2834
61. Yang-Yen, H. F., Chambard, J. C., Sun, Y. L., Smeal, T., Schmidt, T. J., Drouin, J., and Karin, M. (1990) *Cell* **62,** 1205–1215
62. Jones, A., and Doherty, M. (1996) *Ann. Rheum. Dis.* **55,** 829–832
63. Kopp, E., and Ghosh, S. (1994) *Science* **265,** 956–959
64. Gescher, A. (1995) *Toxicol. Lett.* (*Amst.*) **82,** 159–165